



## Three cases of pulmonary tumor thrombotic microangiopathy (PTTM): Challenge in antemortem diagnosis using lung perfusion blood volume images by dual-energy computed tomography

Hiroki Kamada<sup>a,\*</sup>, Hideki Ota<sup>a</sup>, Yosuke Terui<sup>b</sup>, Koichiro Sugimura<sup>b</sup>, Shigefumi Fukui<sup>b</sup>, Hiroaki Shimokawa<sup>b</sup>, Kei Takase<sup>a</sup>

<sup>a</sup> Department of Diagnostic Radiology, Tohoku University Hospital, Sendai, Japan

<sup>b</sup> Department of Cardiovascular Medicine, Tohoku University Graduate School of Medicine, Sendai, Japan

### ARTICLE INFO

#### Keywords:

Pulmonary tumor thrombotic microangiopathy (PTTM)  
Lung perfused blood volume (PBV) images  
Dual-energy computed tomography (CT)  
Pulmonary hypertension

### ABSTRACT

Pulmonary tumor thrombotic microangiopathy (PTTM) is a specific type of tumor embolism in the small and medium pulmonary arteries, leading to rapid progressive pulmonary hypertension. Antemortem diagnosis of PTTM is extremely difficult. We encountered three patients who were histopathologically or clinically diagnosed with PTTM. In all cases, lung perfused blood volume (PBV) images on dual-energy computed tomography (CT) demonstrated multiple subpleural wedge-shaped defects with no evidence of pulmonary embolism on CT pulmonary angiography. The lung PBV images demonstrated small pulmonary arterial obstruction reflecting the pathology of PTTM. Therefore, lung PBV imaging would be useful for antemortem diagnosis of PTTM.

### 1. Introduction

Pulmonary tumor thrombotic microangiopathy (PTTM) is a specific type of pulmonary tumor embolism, which is histopathologically characterized by multiple embolisms and fibrocellular intimal proliferation of small and medium pulmonary arteries [1]. The frequency of PTTM in patients with malignancy has been reported as 1.4–3.3% [2,3]. The major histopathological type associated with PTTM is adenocarcinoma, and the most frequent primary site is the stomach. In contrast, it is less frequent in breast and other cancers [2–5]. PTTM leads to fatal pulmonary manifestations due to rapid progressive pulmonary hypertension and right heart failure [2]. Therefore, it should be considered in the differential diagnosis of rapid progressive and severe cardiopulmonary failure in patients with malignancy. The conventional radiographic features of PTTM are often nonspecific, which impedes its diagnosis during the patient's lifetime. Here, we report lung perfused blood volume (PBV) images obtained by dual-energy computed tomography (CT) in three patients with PTTM.

### 2. Protocol of dual-energy CT

All patients underwent dual-energy CT examinations using a second-generation dual-source CT scanner (SOMATOM Definition

Flash; Siemens Healthcare GmbH, Forchheim, Germany). Image data were acquired with the following scan parameters: voltages/quality effective mAs, 80 kVp/300 mA for tube A and 140 kVp/128 mA for tube B with tin (Sn) filter, gantry rotation speed 0.28 s per rotation; collimation 64 × 0.6 mm; pitch 1.00. Automatic tube current modulation (CareDose4D; Siemens Healthcare GmbH) was enabled.

The scan delay time was fixed to 20 s after the initiation of intravenous contrast media injection. Contrast medium containing 350 mg/mL iodine and saline chaser were injected at 0.075 mL/s/kg body weight from the right antecubital vein in the following injection settings using a double headed power injector (Dual Shot-Type GX; Nemoto-Kyorindo, Tokyo, Japan): (1) contrast medium for the first 16 s, (2) double-diluted contrast medium for the next 4 s (and then scan start), and (3) saline flush for 7 s. The scans of the whole chest were performed in the caudo-cranial direction during a single inspirational breath-hold.

Both the low- and high-energy images were reconstructed at 1-mm thickness with 1-mm increments in the axial plane using soft tissue convolution kernel (D30f). Next, color-coded lung PBV images were reconstructed using a commercially available workstation (syngo CT Workplace; Siemens Healthcare GmbH). The parameters required for material decomposition were employed as manufacturer default setting.

\* Corresponding author. Present address: Department of Diagnostic Radiology, Tohoku University Hospital, 1-1, Seiryomachi, Aoba-ku, Sendai 980-8574, Japan.  
E-mail addresses: [hiroki@pfsi.mech.tohoku.ac.jp](mailto:hiroki@pfsi.mech.tohoku.ac.jp), [hkamada@rad.med.tohoku.ac.jp](mailto:hkamada@rad.med.tohoku.ac.jp) (H. Kamada).

<https://doi.org/10.1016/j.ejro.2020.01.001>

Received 8 December 2019; Received in revised form 14 December 2019; Accepted 5 January 2020

2352-0477/© 2020 The Authors. Published by Elsevier Ltd. This is an open access article under the CC BY-NC-ND license (<http://creativecommons.org/licenses/by-nc-nd/4.0/>).

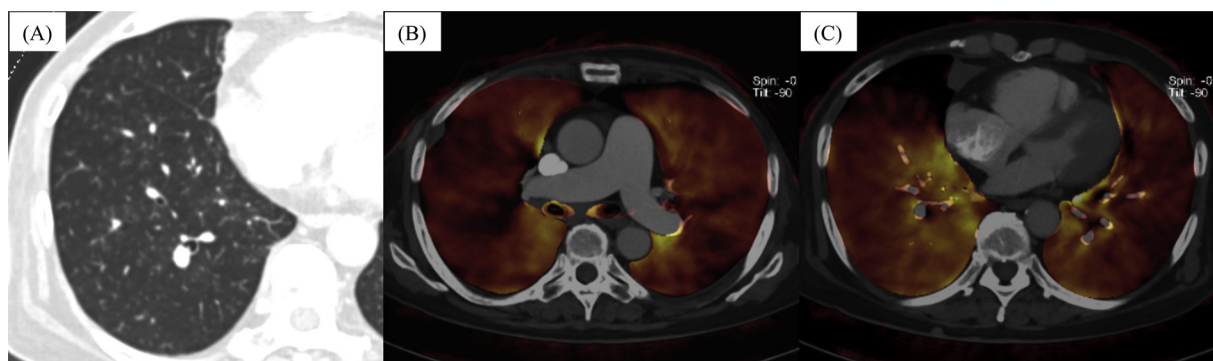


**Fig. 1.** Case 1. A 60-year-old woman. The patient was histopathologically diagnosed with PTTM accompanied by breast cancer at autopsy. (A) Lung CT revealed multiple small bilateral nodules. (B, C) Lung PBV images on dual-energy CT demonstrated bilateral subsegmental defects in the lung.

### 3. Case presentation

#### 3.1. Case 1

A 60-year-old woman with a history of bilateral breast cancer was found to have local recurrence in the right breast, as well as multiple lymph metastases and bone metastases, 1 year ago. Since chemoradiation therapy, brain metastases were newly detected 1 month ago, and she was admitted for whole-brain irradiation. She complained of exertional dyspnea, and a decrease in SpO<sub>2</sub> at rest was detected on day 11. Transthoracic echocardiogram (TTE) revealed tricuspid regurgitation with a pressure gradient (TRPG) of 70 mmHg and pulmonary regurgitation, as well as right atrium/ventricular dilatation, suggesting severe pulmonary hypertension. On day 14, lung CT revealed multiple small bilateral nodules (Fig. 1A). A CT pulmonary angiogram showed no evidence of pulmonary embolism, while the main pulmonary artery was dilated (32 mm in diameter). Lung PBV images obtained by dual-energy CT demonstrated multiple bilateral subpleural wedge-shaped defects in the lung (Fig. 1B and C). The sizes of the local recurrent lesion and lymph metastases showed no remarkable changes compared with CT images taken 1 year previously. She received oxygen administration but died suddenly of respiratory failure on day 15. Autopsy demonstrated multiple embolisms in small and medium pulmonary arteries with fibrocellular intimal proliferation, which were consistent with PTTM.

#### 3.2. Case 2

A 40-year-old woman presented with a 1-month history of dyspnea during exertion and was admitted to our hospital. TTE on day 2 demonstrated tricuspid and pulmonary regurgitation with TRPG of 130 mmHg. Lung CT revealed multiple small bilateral nodules and ground-glass opacities (GGOs) (Fig. 2A and B). The nodules tended to have a centrilobular distribution rather than being located on the interlobular septa. CT pulmonary angiogram showed no evidence of pulmonary embolism (Fig. 2C). Lung PBV images demonstrated small bilateral defects in the pleural margins (Fig. 2D–F). Due to the possibility of PTTM caused by malignancy, gastrointestinal endoscopy and abdominal CT were performed. Gastrointestinal endoscopy detected an ulcer scar on the greater curvature of the gastric body on day 24. A biopsy of the lesion was taken, and it was diagnosed as poorly differentiated gastric adenocarcinoma. Abdominal CT revealed a left ovarian mass, and therefore gadolinium contrast-enhanced magnetic resonance imaging and <sup>18</sup>F-fluorodeoxyglucose (FDG) positron emission tomography (PET)/CT were additionally performed. Contrast-enhanced magnetic resonance imaging on day 24 indicated that the left ovarian cystic lesion included a solid component with diffusion restriction and enhancement. On PET/CT, abnormal FDG uptake was not found along the gastric wall, whereas FDG uptake was demonstrated in the solid

component of the left ovarian lesion as well as in small nodules and GGOs of the bilateral lungs. These findings suggested gastric adenocarcinoma with left ovarian metastasis, which would result in PTTM. The patient underwent chemotherapy with cisplatin. She received percutaneous cardiopulmonary support, and took pulmonary vasodilators including epoprostenol, macitentan, and tadalafil. On day 51, her respiratory status was improved, and the patient was transferred to another hospital for further chemotherapy and follow-up of PTTM.

#### 3.3. Case 3

A 50-year-old woman with a history of left breast cancer had multiple bone and lung metastases detected 6 months ago. Since chemoradiation therapy, she had multiple liver and brain metastases newly detected 1 month ago and was admitted for additional chemoradiation therapy. She had dyspnea that was gradually worsening since 1 month ago. On admission, she complained of severe dyspnea with a decrease in SpO<sub>2</sub> at rest. TTE revealed TRPG of 52 mmHg and right atrium/ventricular dilatation, which suggested moderate pulmonary hypertension. Contrast-enhanced lung CT showed no evidence of pulmonary embolism or lymphangitic carcinomatosis. Lung PBV images by dual-energy CT demonstrated multiple bilateral wedge-shaped defects in the lung (Fig. 3). She received oxygen administration but died of respiratory failure on day 2. The patient was diagnosed with PTTM based on the clinical course and the results of imaging studies.

### 4. Discussion

We encountered three patients with severe and progressive pulmonary hypertension and right heart failure. The first patient was histopathologically diagnosed with PTTM accompanied by breast cancer at autopsy, the second had suspected PTTM due to gastric adenocarcinoma that showed improvement with chemotherapy, and the third was clinically diagnosed with PTTM associated with breast cancer metastases. In all cases, lung PBV images demonstrated multiple subpleural wedge-shaped defects with no evidence of pulmonary embolism on CT pulmonary angiography. The findings suggested small pulmonary arterial obstructions, which could reflect the pathology of PTTM.

A diagnosis of PTTM is extremely difficult as various causes of right heart failure and pulmonary hypertension have similar clinical presentations, and therefore most cases are diagnosed postmortem [6]. Histopathological evaluation is required for a definitive diagnosis of PTTM. Previous reports have suggested the usefulness of CT-guided needle biopsy, transbronchial lung biopsy, and cytology of wedge pulmonary arterial blood cell sampling [3,4,7]. These techniques, however, are invasive and risky in cases with right heart failure and pulmonary hypertension. In our cases, patients declined tissue biopsy of the lung, and radiological examinations, including dual-energy CT,

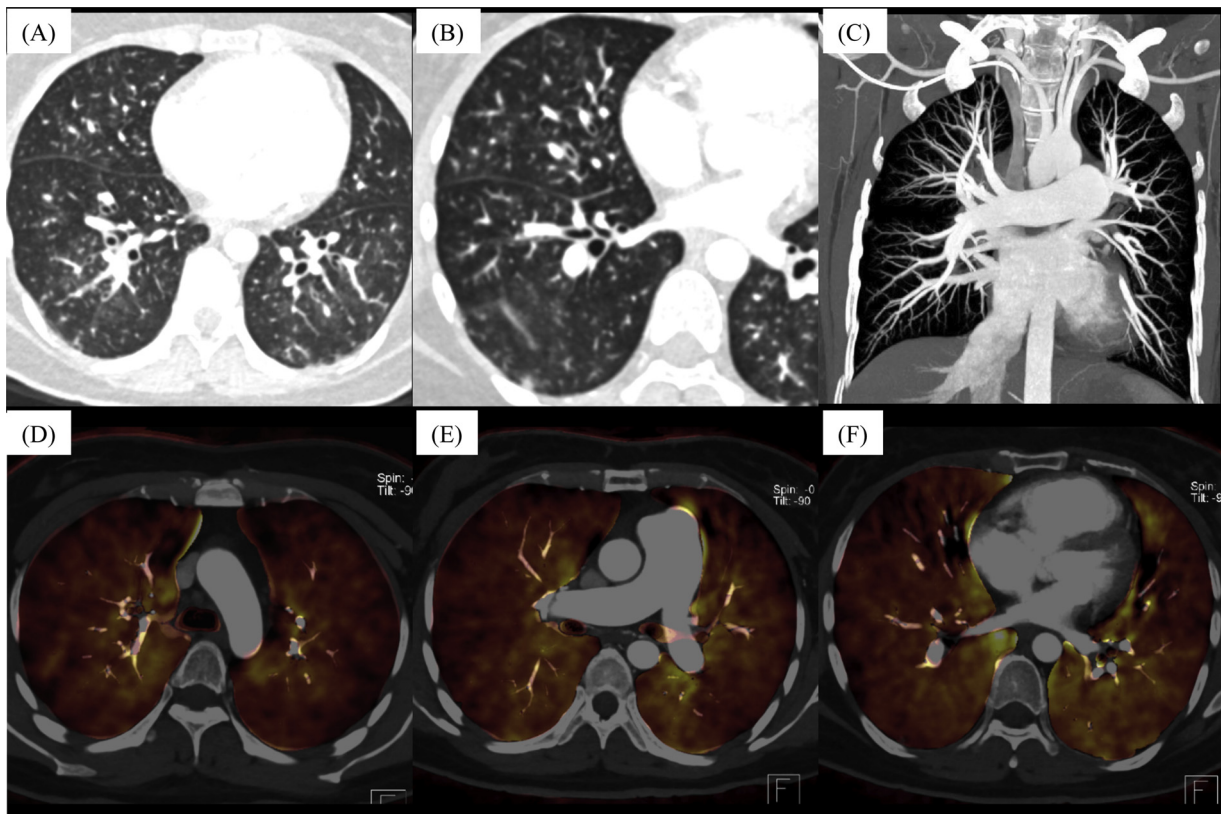


**Fig. 2.** Case 2. A 40-year-old woman with suspected PTTM due to gastric adenocarcinoma and improvement on chemotherapy. (A, B) Lung CT revealed multiple small bilateral nodules and ground-glass opacities (GGOs). (C) A CT pulmonary angiogram showed no evidence of pulmonary embolism. (D–F) Lung PBV images demonstrated small bilateral defects in the pleural margins.

were conducted to assess the pulmonary artery and lung.

Conventional radiographic findings of PTTM are nonspecific and unremarkable [6,8]. Lung CT reveals nodule features, GGO, septal thickening, consolidation, and mediastinal/hilar lymphadenopathy [6,8]. These morphological abnormalities are interpreted by pulmonary hypertension and right heart failure but contribute less to diagnosis.

Lung perfusion scintigraphy can detect peripheral perfusion defects, and its usefulness for the diagnosis of PTTM has been reported [3,4,9,10]. Recently, lung PBV imaging by dual-energy CT has been developed to evaluate the distribution of blood perfusion in the lung. Lung PBV is iodine-specific image based on two CT datasets acquired

with different X-ray spectra [11]. Lung PBV was useful for evaluation of pulmonary perfusion defects, with good agreement with lung perfusion scintigraphy [12]. To our knowledge, there have been no previous reports of lung PBV findings in PTTM. The findings of lung PBV in our cases demonstrated multiple bilateral subpleural defects that appeared similar to the findings on lung perfusion scintigrams. In fact, one case in our study had both lung PBV and perfusion scintigraphy findings that were consistent with each other. Here, clinical information should be taken into account along with the CT findings for PTTM because the differential diagnosis includes other peripheral pulmonary vessel diseases, as exemplified by chronic thromboembolic pulmonary

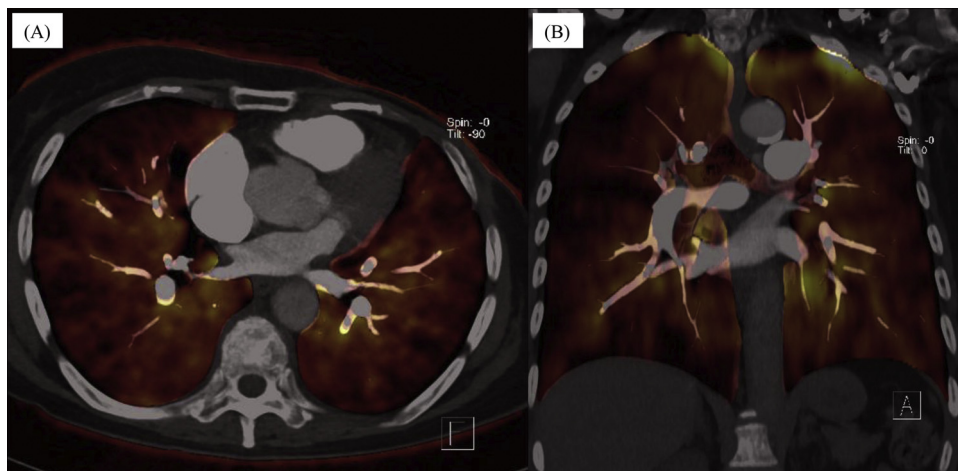


**Fig. 3.** Case 3. A 50-year-old woman clinically diagnosed with PTTM associated with breast cancer metastases. Lung PBV images demonstrated small bilateral defects in the pleural margins on (A) axial and (B) coronal sections.

hypertension and pulmonary veno-occlusive disease. However, the lack of steno-occlusive lesions on CT pulmonary angiography in PTTM may become a key finding to exclude chronic thromboembolic pulmonary hypertension.

The use of FDG PET/CT for diagnosis of PTTM has been reported [3], and a case report by Tashima et al. [13] demonstrated multiple foci with FDG uptake in both lungs in PTTM. In our case, abnormal FDG uptake was observed in the GGOs of the lung. Nevertheless, it was not clear whether it was a tumor embolism because abnormal uptake in the gastric wall was not obvious, implying the less FDG-avid histopathological subtype [14]. Moreover, the presence of uptake could not exclude coexisting pulmonary inflammation.

## 5. Conclusion

Antemortem diagnosis of PTTM is challenging. Clinically, PTTM should be considered in the differential diagnosis of rapid progressive and severe cardiopulmonary failure in patients with diagnosed or suspected malignancy. In diagnostic radiology, lung PBV imaging by dual-energy CT can detect multiple bilateral subpleural defects regardless of the lack of steno-occlusive lesions on CT pulmonary angiography, and it would be useful for antemortem diagnosis of PTTM.

## Declaration of Competing Interest

None.

## References

- [1] J.K. Pinckard, M.R. Wick, Tumor-related thrombotic pulmonary microangiopathy: review of pathologic findings and pathophysiologic mechanisms, *Ann. Diagn. Pathol.* 4 (2000) 154–157.
- [2] A. von Herbay, A. Illes, R. Waldherr, H.F. Otto, Pulmonary tumor thrombotic microangiopathy with pulmonary hypertension, *Cancer* 66 (1990) 587–592.
- [3] H. Uruga, T. Fujii, A. Kurosaki, S. Hanada, H. Takaya, A. Miyamoto, N. Morokawa, S. Homma, K. Kishi, Pulmonary tumor thrombotic microangiopathy: a clinical analysis of 30 autopsy cases, *Intern. Med.* 52 (2013) 1317–1323.
- [4] T. Abe, I. Fukada, T. Shiga, H. Morizono, K. Ikebata, T. Shibayama, K. Kobayashi, T. Iwase, S. Ohno, Y. Ito, A case of recurrent breast cancer Identified by pulmonary tumor thrombotic microangiopathy, *Case Rep. Oncol.* 10 (2017) 620–626.
- [5] M. Story, S.K. Kwon, R. Robinson, S. Fortis, Acute cor pulmonale due to pulmonary tumour thrombotic microangiopathy from renal cell carcinoma, *BMJ Case Rep.* (2017), <https://doi.org/10.1136/bcr-2017-219730> pii: bcr-2017-219730.
- [6] R.H. Godbole, R. Saggar, N. Kamangar, Pulmonary tumor thrombotic microangiopathy: a systematic review, *Pulm. Circ.* 9 (2019), <https://doi.org/10.1177/2045894019851000> 2045894019851000.
- [7] A. Tateishi, K. Nakashima, K. Hoshi, Y. Oyama, T. Ebisudani, M. Misawa, M. Aoshima, Pulmonary tumor thrombotic microangiopathy mimicking inhalation lung injury, *Intern. Med.* 58 (2019) 1311–1314, <https://doi.org/10.2169/internalmedicine.1796-18>.
- [8] L.C. Price, A.U. Wells, S.J. Wort, Pulmonary tumour thrombotic microangiopathy, *Curr. Opin. Pulm. Med.* 22 (2016) 421–428, <https://doi.org/10.1097/MCP.0000000000000297>.
- [9] H. Toyonaga, M. Tsuchiya, C. Sakaguchi, H. Ajimizu, Y. Nakanishi, S. Nishiyama, N. Morikawa, Y. Hayashi, Y. Nagasaka, H. Yasui, Pulmonary tumor thrombotic microangiopathy caused by a parotid tumor: early antemortem diagnosis and long-term survival, *Intern. Med.* 56 (2017) 67–71, <https://doi.org/10.2169/internalmedicine.56.7439> Epub 2017 Jan 1.
- [10] S. Miyazaki, T. Ikeda, G. Ito, M. Inoue, K. Nara, Y. Nishinaga, Y. Hasegawa, Pulmonary tumor thrombotic microangiopathy successfully treated with corticosteroids: a case report, *J. Med. Case Rep.* 11 (2017) 356, <https://doi.org/10.1186/s13256-017-1524-8>.
- [11] T.R. Johnson, Dual-energy CT: general principles, *AJR Am. J. Roentgenol.* 199 (2012) S3–S8, <https://doi.org/10.2214/AJR.12.9116>.
- [12] S.F. Thieme, C.R. Becker, M. Hacker, K. Nikolaou, M.F. Reiser, T.R. Johnson, Dual energy CT for the assessment of lung perfusion—correlation to scintigraphy, *Eur. J. Radiol.* 68 (2008) 369–374, <https://doi.org/10.1016/j.ejrad.2008.07.031> Epub 2008 Sep 5.
- [13] Y. Tashima, K. Abe, Y. Matsuo, S. Baba, K. Kaneko, T. Isoda, H. Yabuuchi, M. Sasaki, H. Honda, Pulmonary tumor thrombotic microangiopathy: FDG-PET/CT findings, *Clin. Nucl. Med.* 34 (2009) 175–177, <https://doi.org/10.1097/RLU.0b013e3181966f5c>.
- [14] A. Stahl, K. Ott, W.A. Weber, K. Becker, T. Link, J.R. Siewert, M. Schwaiger, U. Fink, FDG PET imaging of locally advanced gastric carcinomas: correlation with endoscopic and histopathological findings, *Eur. J. Nucl. Med. Mol. Imaging* 30 (2003) 288–295 Epub 2002 Nov 8.